In vivo stabilization of a less toxic asparaginase variant leads to a durable antitumor response in acute leukemia

Maaike Van Trimpont,[1,2,3] Amanda M. Schalk,[4] Yanti De Visser,[1,2,5] Hien Anh Nguyen,[4] Lindy Reunes,[1,2] Katrien Vandemeulebroecke,[1,6,7] Evelien Peeters,[1,3] Ying Su,[4] Hyun Lee,[8,9] Philip L. Lorenzi,[10] Wai-Kin Chan,[10] Veerle Mondelaers,[1,6] Barbara De Moerloose,[1,6,7] Tim Lammens,[1,6,7] Steven Goossens,[1,3] Pieter Van Vlierberghe[1,2#] and Arnon Lavie[4,11#]

[1]Cancer Research Institute Ghent (CRIG), Ghent, Belgium; [2]Department of Biomolecular Medicine, Ghent University, Ghent, Belgium; [3]Department of Diagnostic Sciences, Ghent University, Ghent, Belgium; [4]Department of Biochemistry and Molecular Genetics, University of Illinois at Chicago, Chicago, IL, USA; [5]Department of Imaging and Pathology, KU Leuven, Leuven, Belgium; [6]Department of Pediatric Hemato-Oncology and Stem Cell Transplantation, Ghent University Hospital, Ghent, Belgium; [7]Department of Internal Medicine and Pediatrics, Ghent University, Ghent, Belgium; [8]Department of Pharmaceutical Sciences, College of Pharmacy, University of Illinois at Chicago (UIC), Chicago, IL, USA; [9]Biophysics Core at Research Resources Center, University of Illinois at Chicago (UIC), Chicago, IL, USA; [10]Metabolomics Core Facility, Department of Bioinformatics and Computational Biology, The University of Texas MD Anderson Cancer Center, Houston, TX, USA and [11]The Jesse Brown VA Medical Center, Chicago, IL, USA.

#PVV and AL contributed equally as co-senior authors

Correspondence: A. Lavie
Lavie@uic.edu

Received: May 11, 2022.
Accepted: August 4, 2022.
Prepublished: August 18, 2022.

https://doi.org/10.3324/haematol.2022.281390

In vivo stabilization of a less toxic asparaginase variant leads to a durable anti-tumor response in acute leukemia

Maaike Van Trimpont[1,2,3], Amanda M. Schalk[4], Yanti De Visser[1,2,5], Hien Anh Nguyen[4], Lindy Reunes[1,2], Katrien Vandemeulebroecke[1,6,7], Evelien Peeters[1,3], Ying Su[4], Hyun Lee[8,9], Philip L. Lorenzi[10], Wai-Kin Chan[10], Veerle Mondelaers[1,6], Barbara De Moerloose[1,6,7], Tim Lammens[1,6,7], Steven Goossens[1,3], Pieter Van Vlierberghe[1,2**] and Arnon Lavie[4,11**]

Supplementary Appendix

Supplementary Figures

Supplementary Figure S1

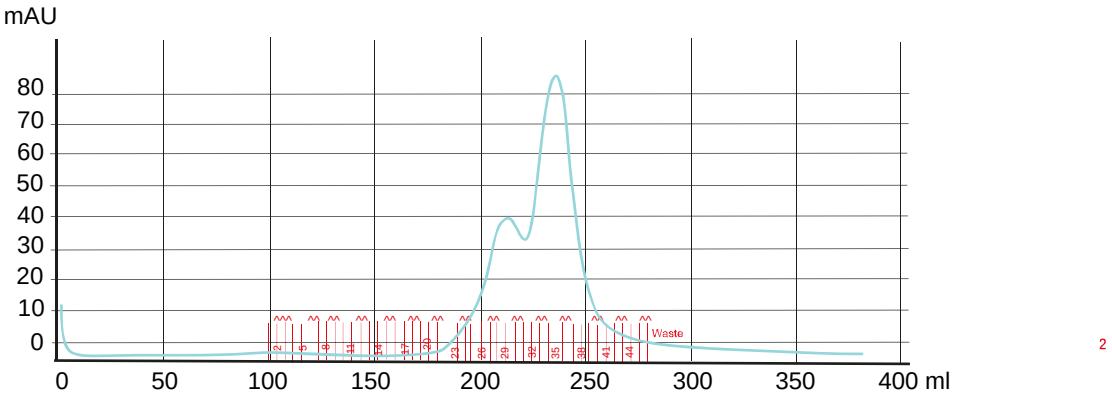

Supplementary Figure S1: Size exclusion chromatogram for ABD-*Er*A-TM. This figure shows the size exclusion chromatogram for ABD-*Er*A-TM and has two peaks, one that corresponds to the expected size of the octamer, and a larger peak that the corresponds to the expected size of the tetramer.

Supplementary Figure S2

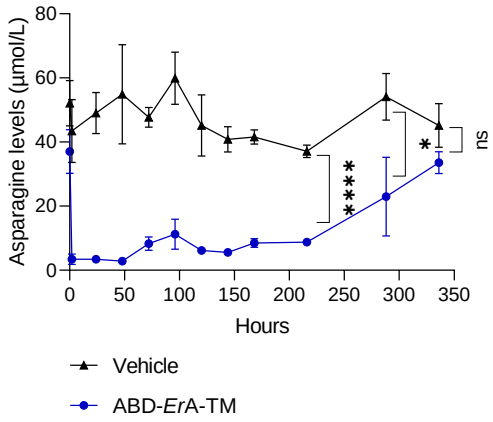

Supplementary Figure S2: ABD-*Er*A-TM has the ability to deplete asparagine levels. A significant decrease in asparagine levels is observed after a single administration/dose of ABD-*Er*A-TM (2500 IU/kg, intraperitoneally injection) compared to vehicle treated mice (2 – 216 hours $p<0.0001$; 288 hours $p=0.0195$; Student's unpaired t-test) clearly showing that our alternative, low-glutaminase variant is capable of lowering asparagine levels in the blood.

Supplementary Figure S3

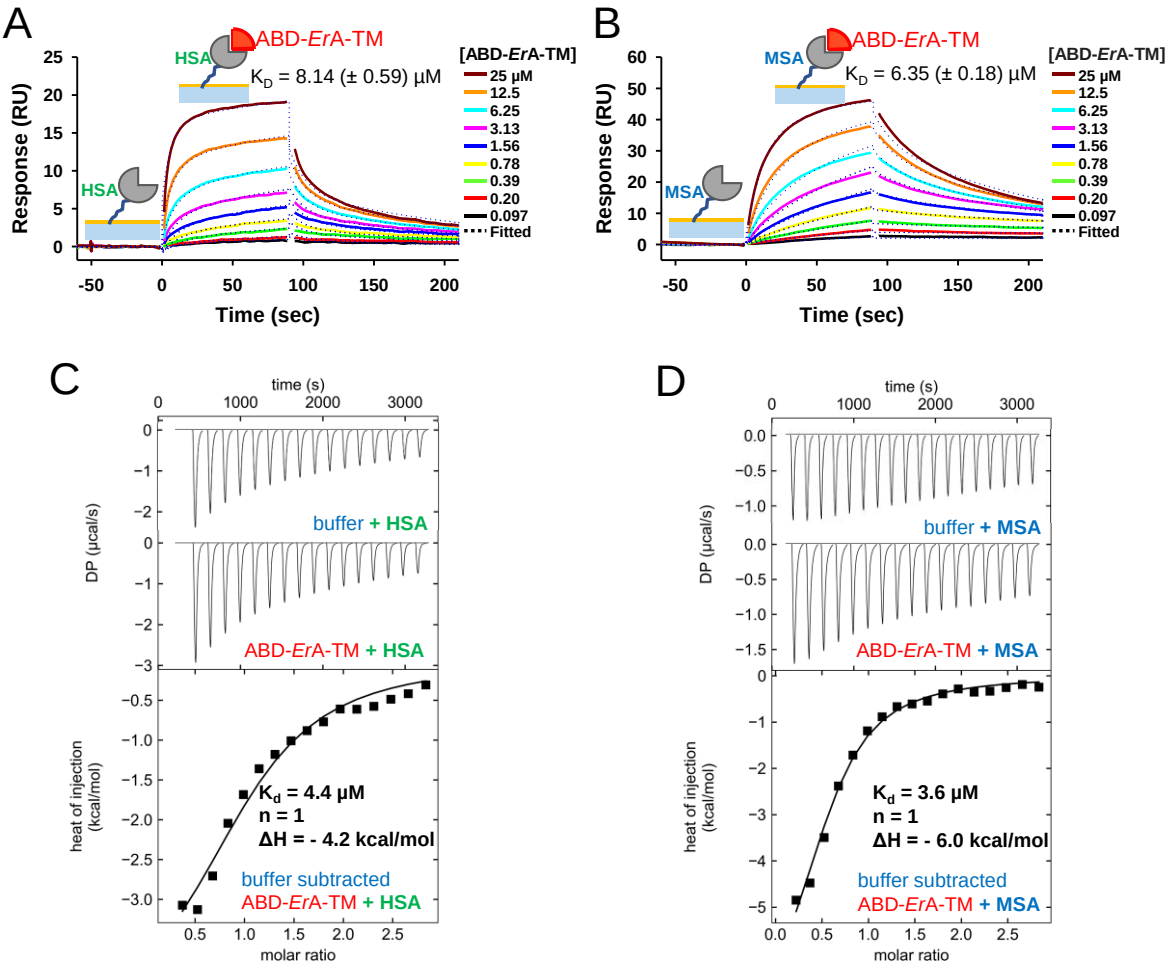

Supplementary Figure S3: ABD-*Er*A-TM interacts with human serum albumin (HSA) and mouse serum albumin (MSA). To verify that our ABD-*Er*A-TM molecule binds serum albumins, we used Surface Plasmon Resonance (SPR) to determine the *in vitro* interaction. Sensorgrams of ABD-*Er*A-TM binding to the immobilized HSA **A)** and MSA **B)**. A series of increasing concentrations (0.097 – 25 µM at 2-fold dilution) of ABD-*Er*A-TM were applied. The equilibrium dissociation constants (K_D) were determined from two rate constants ($K_D = k_d/k_a$). Standard deviations were calculated from four measurements. Isothermal titration calorimetry (ITC) experiments confirm interaction between ABD-*Er*A-TM and two serum albumins. Representative ITC raw data (top and middle) and binding isotherm (bottom) for HSA **C)** and MSA **D)** interacting with ABD-*Er*A-TM.

Supplementary Figure S4

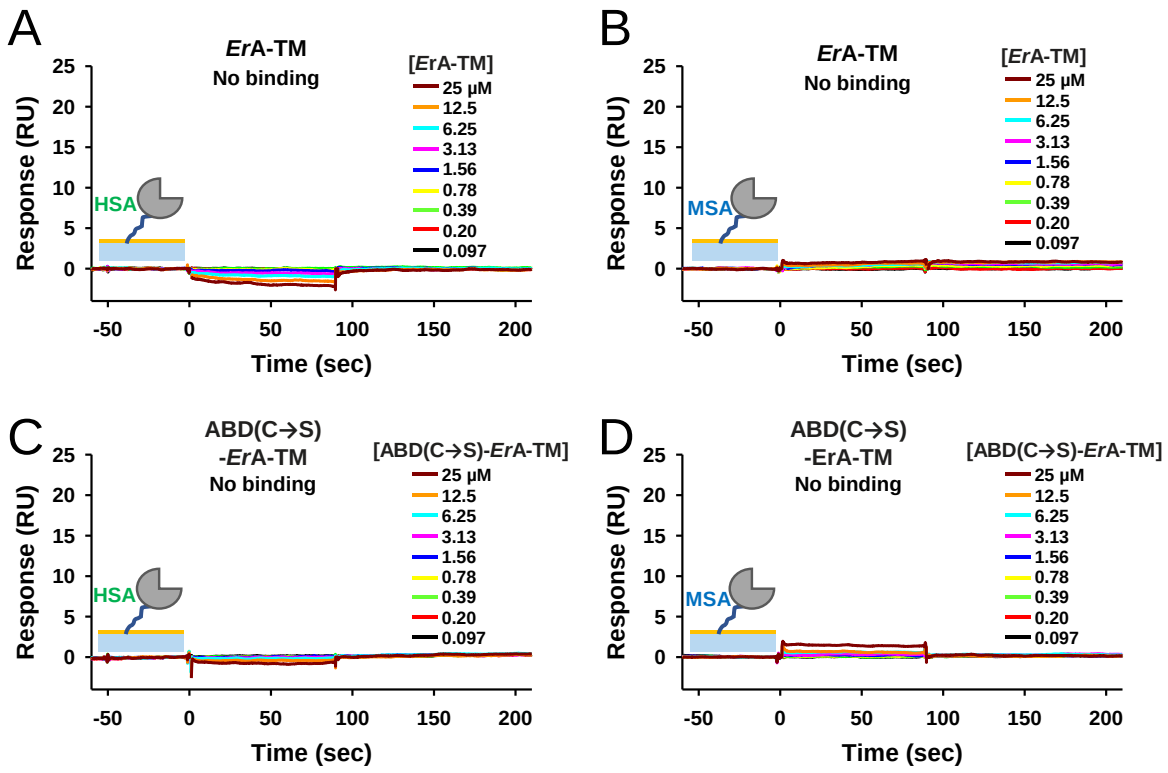

Supplementary Figure S4: *Er*A-TM and ABD-(C->S)-*Er*A-TM do not interact with human serum albumin (HSA) and mouse serum albumin (MSA). To verify that our *Er*A-TM and ABD(C->S)-*Er*A-TM molecules bind serum albumins, we used Surface Plasmon Resonance (SPR) to determine the *in vitro* interaction. Sensorgrams of *Er*A-TM binding to the immobilized HSA **A)** and MSA **B)** Sensorgrams of ABD(C->S)-*Er*A-TM binding to the immobilized HSA **C)** and MSA **D)** A series of increasing concentrations (0.097 – 25 µM at 2-fold dilution) of each analyzing protein were applied. No binding was observed for both *Er*A-TM and ABD(C->S)-*Er*A-TM.

Supplementary Figure S5

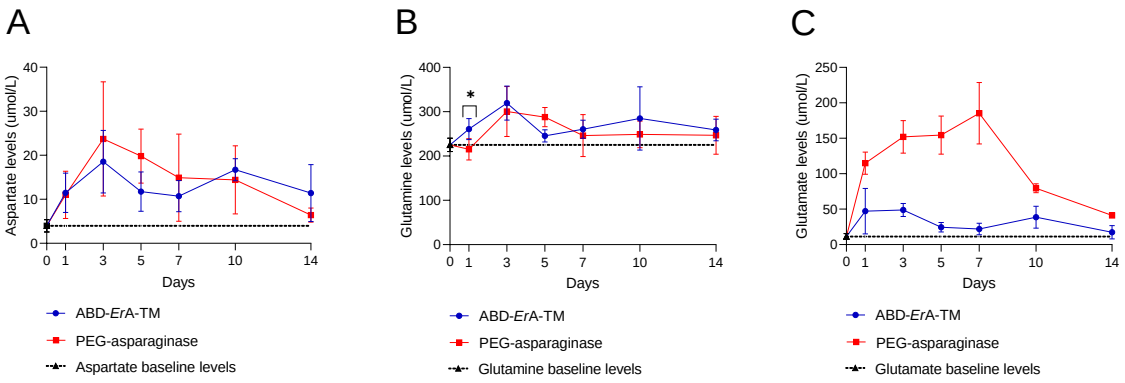

Supplementary Figure S5: Similar *in vivo* ability for ABD-*Er*A-TM and PEG-asparaginase to deplete blood asparagine but dissimilar impact on glutamine homeostasis. For each time point, the mean and SD are shown (n=5 for each group). **A)** Determination of aspartate levels in blood plasma samples of mice prior to the treatment and at days 1, 3, 5, 7, 10 and 14 post administration of ABD-*Er*A-TM and PEG-asparaginase. Plasma aspartate levels increased significantly at days 1 and 3 (p=0.0079 ; Mann-Whitney *U* test) compared to baseline levels and then decreased to the pretreatment level by day 14 for both treatment groups **B)** Determination of glutamine levels in blood plasma samples of mice prior to the treatment and at days 1, 3, 5, 7, 10 and 14 post administration of ABD-*Er*A-TM and PEG-asparaginase. At 24h, a significant difference in glutamine levels between both treatment groups is observed (p=0.0317 ; Mann-Whitney *U* test) **C)** Determination of glutamate levels in blood plasma samples of mice prior to the treatment and at days 1, 3, 5, 7, 10 and 14 post administration of ABD-*Er*A-TM and PEG-asparaginase. For the PEG-asparaginase mice, a significant increase in glutamate is observed compared to ABD-*Er*A-TM treated mice (day 1 – day 14 p=0.0079 ; Mann-Whitney *U* test).

Supplementary Figure S6

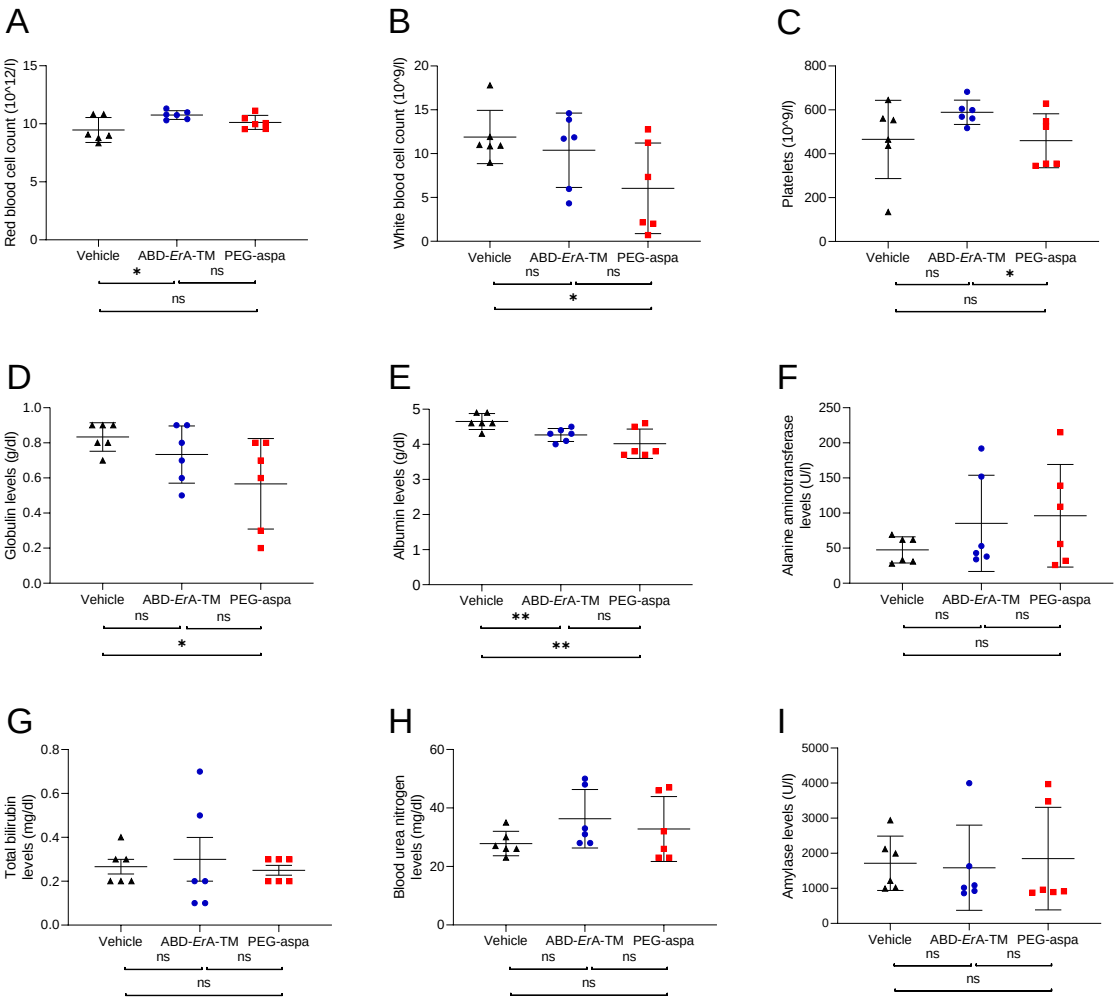

Supplementary Figure S6: Toxic effect of a single 2500 IU/kg administration/dose ABD-*Er*A-TM or PEG-asparaginase on hematological and biochemical parameters in mice. For each figure, the mean and SD are shown (n=6 for each group). Statistical analysis was performed applying Mann-Whitney tests and a Bonferroni adjusted alpha-level **A)** Average red blood cell count shows no significant difference between ABD-*Er*A-TM treated and PEG-asparaginase treated mice **B)** Average white blood cell count decreased more in PEG-asparaginase mice than in ABD-*Er*A-TM mice compared to vehicle PBS mice. **C)** When comparing the average blood platelet levels from PEG-asparaginase treated mice (459.33 x 10^9/L) to the ABD-*Er*A-TM group (588.83 x 10^9/L), a decrease is observed, although not significant **D)** Globulin levels were slightly reduced in PEG-asparaginase mice **E)** Albumin levels were reduced in both PEG-asparaginase and ABD-*Er*A-TM mice compared to vehicle mice (p=0.0084 and p=0.0094 respectively) **F-I)** Biochemical analysis shows no significant differences between vehicle, ABD-*Er*A-TM or PEG-asparaginase treated mice for **F)** alanine aminotransferase **G)** total bilirubin **H)** blood urea nitrogen **I)** amylase

Supplementary Figure S7

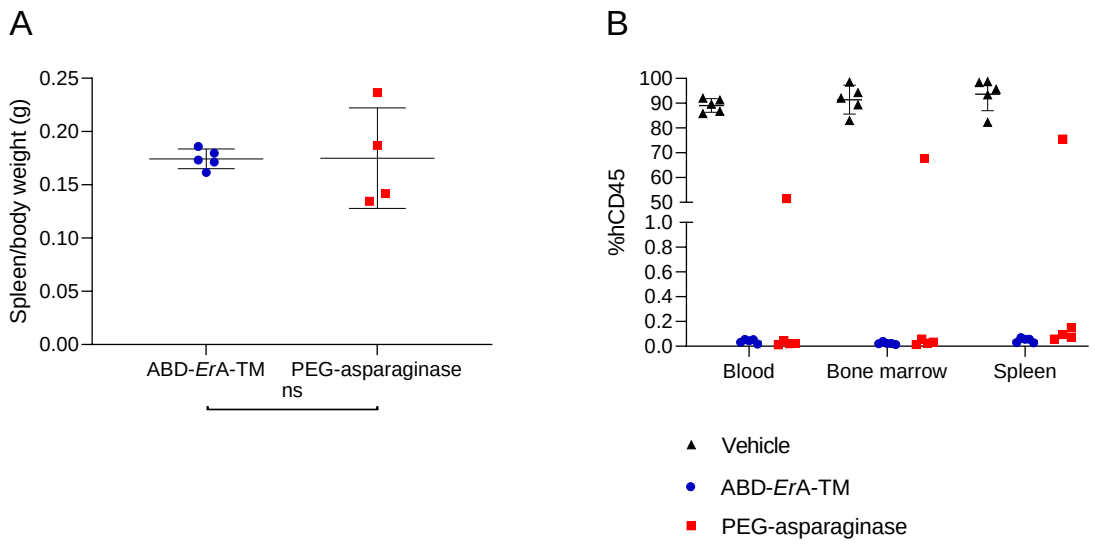

Supplementary Figure S7: Endpoint analysis shows no signs of leukemic burden. **A)** At the end of the survival experiment, no significant difference in spleen/body weight between both treatment groups was observed ($p>0.05$; Mann-Whitney *U* test) **B)** Analysis of human CD45+ cells in peripheral blood, spleen and bone marrow showed undetectable levels of leukemic cells in both PEG-asparaginase and ABD-*Er*A-TM mice, with exception of one PEG-asparaginase that relapsed during survival analysis

Supplementary Table

Supplementary Table S1

Structure	**ABD-*Er*A-TM**
PDB codes	7U6M
Data collection statistics	
X-ray source and detector	LS-CAT EIGER 1M
Wavelength (Å)	1.12723
Temperature (K)	100
Resolution[a] (Å)	1.75 (1.80-1.75)
Number of Reflections [a]	
Observed	5,007,802 (387,732)
Unique	316,581 (25,735)
Completeness (%) [a]	99.9 (100.0)
R_{sym} (%) [b]	17.7 (198.1)
CC(1/2) [b]	99.6 (80.0)
Average I/σ(I) [a]	8.62 (2.17)
Space group	$P2_12_12_1$
Unit cell (Å): a, b, c	80.2, 130.4, 155.1
Wilson B-factor (Å^2)	41.2
Refinement statistics	
Refinement program	REFMAC5
R_{cryst} (%)	14.54
R_{free} (%)	16.56
Resolution range (Å)	20.0-1.75
Protein molecules per a.u.	4
Number of atoms	
Protein (ProtA, protB, protC, protD)	 2491, 2539, 2626, 2502
Water molecules	1148
Asp molecules	4
Ramachandran plot statistics (%) Most favored regions	91.6
Additionally allowed regions	8.0
Outlier regions	0.4

[a] High resolution shell in parenthesis

Table S1: Data collection and refinement statistics for ABD-*Er*A-TM

Supplementary Methods

Expression and purification of ABD-ErA-TM and ABD-ErA-WT

ABD-*Er*A-TM and ABD-*Er*A-WT (WT=wild-type; in effect, Erwinaze fused to ABD) were expressed as His-SUMO fusion proteins in *E. coli* grown at 18°C overnight after induction with 0.3 mM isopropyl β-d-1-thiogalactopyranoside (IPTG). After capture of the His-tagged protein using a His-TRAP column, non-specifically bound proteins were eluted with nickel affinity buffer (25 mM Tris pH 7.9, 500 mM NaCl) containing first 30 mM and then 60 mM imidazole. To elute endotoxins, the column-bound protein was washed overnight with ~750 mL of nickel affinity buffer containing 0.1% Triton X-114. The following morning, Triton X-114 was removed by washing with the nickel affinity buffer. For elution of His-SUMO-ABD-*Er*A-TM/WT, nickel affinity buffer was augmented with 500 mM imidazole, 2 mM TCEP, 1 mM betamercaptoethanol, 100 mM glycine. The His-SUMO tag was cleaved from the eluted fusion proteins using SUMO protease (ratio 1:200) at room temperature overnight. About 50% of the protein precipitates in this cutting step, presumably due to incorrect disulfide bond formation. After spinning and filtering the protein, it is then injected onto a Hi-Prep S-200 gel filtration column (Cytiva) equilibrated with 25 mM Tris, pH 7.5, 150 mM NaCl, and 50 mM glycine and run at 2 mL/min. Just prior to the elution volume, two 5 mL CAPTO DEAE anion exchange columns (Cytiva) are connected to the outlet of the gel filtration column, and the flow rate is reduced to 0.5 mL. This is done as a secondary method to reduce the endotoxin level. As a final method to reduce endotoxins, the fractions containing ABD-*Er*A-TM/WT are incubated overnight in Detoxi-Gel (ThermoFisher), followed by concentration to 5 mg/mL before being aliquoted and frozen in liquid nitrogen for storage at -80°C. Endotoxin levels were measured using a Charles River Laboratories Endosafe nexgen-PTS system.

Crystal structure of ABD-ErA-TM

ABD-*Er*A-TM at 5 mg/mL in the presence of 5 mM aspartic acid was crystallized using the hanging drop method at room temperature in 12-17% PEG 3350, 0.1 ammonium citrate, pH 7.0, by mixing 2 µL of protein with 1 µL of reservoir solution. Diffraction data were collected at the Life Sciences Collaborative Access Team (LS-CAT) beamline at the Advanced Photon Source. The final data set was merged from 4 crystals. The structure was solved by molecular replacement (Molrep) using PDB ID 5I48 as the search model. Refinement was done using Refmac and model fitting to the electron density was done using Coot. See Table S1 for data collection and refinement statistics.

Surface Plasmon Resonance (SPR)

The human serum albumin (HSA) and mouse serum albumin (MSA) proteins were purchased from MilllporeSigma (Cat #: 126658) and Molecular Innovations (Cat #: MSA-121-100mg). The expression and purification of *Er*A-TM was done as previously described[1]. HSA and MSA were initially prepared in buffer containing 20 mM phosphate, pH 7.4, 137 mM NaCl, 2.7 mM KCl, 0.05% Tween-20. The CM5 sensor surface was first activated by 1-ethyl-3-(3-dimethylaminopropyl) carbodiimide hydrochloride (EDC)/N-hydroxysuccinimide (NHS) mixture using a Biacore T200 instrument (Cytiva, former GE Healthcare). Two proteins, HSA and MSA, were diluted to 50 µg/mL in 10 mM sodium acetate at pH 4.5 and immobilized to flow channels 2 and 4 on the CM5 chip followed by ethanolamine blocking on the unoccupied surface area. Flow channels 1 and 3 were activated by EDC/NHS and deactivated by ethanolamine and used as references. Three analyzing protein solutions were initially in 25 mM Tris, pH 8.5, 155 mM NaCl, and 100 mM Glycine and buffer exchanged with a SPR binding buffer (25 mM HEPES, pH 7.2, 200 mM NaCl, 0.05% Tween-20). A series of increasing concentrations (0.097 – 25 µM at 2-fold dilution) of each analyzing protein was applied to all four channels with 90 seconds association and 180 second dissociation times at a 30 µL/min flow rate at 25°C. The data was double referenced with reference channel and zero concentration responses, and reference subtracted sensorgrams were fitted with 1 to 1 Langmuir kinetic model using a Biacore T200 evaluation software V3.0. The equilibrium dissociation constants (KD) were determined from two rate constants (KD = kd/ka).

Isothermal Titration Calorimetry (ITC)

The ABD-*Er*A-TM protein was prepared in ITC buffer (25 mM HEPES, pH 7.2, 200 mM NaCl, 0.05% Tween 20) at 25 µM concentration and placed in the sample cell of the VP-ITC titration microcalorimeter from MicroCal™, LLC (Northampton, MA). All ITC experiments were performed while stirring at 351 rpm, in ITC buffer at 25°C. HSA and MSA solutions were prepared in the same ITC buffer at 350 µM and loaded onto the microsyringe. All titrations were conducted using an initial injection of 7.5 µL followed by 18 identical injections of 15 µL with a duration of 16 sec (per injection) and a spacing of 240 sec between injections. The buffer control titration (HSA or MSA into ITC buffer) signals were subtracted from the experimental data. The collected data were evaluated using NITPIC (NIH), SEDPHAT (NIH), and GUSSI (NIH).

Enzyme activity assay

The catalytic activities of the L-ASNase variants were determined using a continuous spectroscopic enzyme-coupled assay. These assays measured the production of the end

products of the L-ASNase reaction (Asp and ammonia) through the 1:1 oxidation of reduced NADH to NAD, which is observed spectroscopically as a decrease in absorbance at 340 nm where glutamic-oxalacetic transaminase (Sigma G2751) and malic dehydrogenase (Sigma M2634) are utilized as the helper enzymes[2, 3]. The kinetic assay buffer was comprised of 25 mM Tris, pH 8.0, 300 mM NaCl, 400 µM alpha-ketoglutarate, and 200 µM NADH. A stock solution of Asn (Sigma-Aldrich A93003) in 25 mM Tris pH 7.5, 155 mM NaCl was made fresh and used to trigger the reaction. Rates were measured at 37°C at a constant ASNase concentration of 0.2 nM enzyme, which was selected to obtain rates that were linear. Varying concentrations of Asn ranging from 25 µM to 4 mM were used to the obtain kcat and Km values. All measurements were taken in triplicate. SigmaPlot software was used to fit kobs rates to the Michaelis-Menten equation.

In vivo ABD-ErA-TM and PEG-asparaginase pharmacokinetics and pharmacodynamics study

For the *in vivo* pharmacodynamic pilot study, 10-week-old NSG mice (#005557, the Jackson Laboratory) were treated intraperitoneally with ABD-*Er*A-TM or PEG-asparaginase at a dose of 2,500 IU/kg bodyweight. Phosphate buffered saline was used as a vehicle control. At time points 0h (before treatment), 2h, 24h, 48h, 72h, 96 h, 120h, 144h, 168h, 216h, 288h and 336h, 5 µL whole blood was collected from the tail vein. The collected sample was immediately neutralized with 30 µL of methanol containing 1% formic acid and vortex-mixed briefly. The samples were then stored at -80°C until analysis by LC-MS/MS for the measurement of Asn as reported previously.

For the other pharmacodynamic and pharmacokinetic study, healthy wild type C57BL/6J (female mice (n=35) between the ages of 9-22 weeks were randomly divided into a vehicle phosphate buffered saline (PBS) (n=5), PEG-asparaginase (n=15) and ABD-*Er*A-TM (n=15) treatment group. One single administration/dose of 2500 IU/kg PEG-asparaginase or ABD-*Er*A-TM was administered via intraperitoneal injection. Vehicle mice received the same volume of PBS. Peripheral blood was collected via a cut in the tail vein at day 0 and 7 for all 3 groups, while additional samples were taken for the PEG-asparaginase and ABD-*Er*A-TM treated mice at days 1, 3, 10 and 14 post L-ASNase administration. At each time point, blood was collected from 5 mice in each group.

Due to limitations in the maximum allowed blood volume that can be taken weekly from mice, we provided 15 mice per treatment group and rotated between the mice to ensure optimal comfort. For the PEG-asparaginase treated mice at the 24h time point, blood for pharmacokinetics had to be pooled from different mice, as we did not have enough sample for both pharmacokinetics and pharmacodynamics. For the activity determinations, 50 µL of

peripheral blood was collected and samples were processed according to the protocol described by Nguyen *et al*.[4] For the amino acid (AA) level determinations, 120 µL of peripheral blood was collected and AAs were measured as previously described[4].

Single dose acute toxicity study

In this single dose acute toxicity study, healthy wild type C57BL/6J (Charles River) female mice (9 weeks old; n=18) were randomly divided into a vehicle PBS (n=6), PEG-asparaginase (n=6) and ABD-*Er*A-TM (n=6) treatment group. One single administration/dose of PEG-asparaginase or ABD-*Er*A-TM was administered via intraperitoneal injection at a dose of 2500 IU/kg. Vehicle PBS mice received the same volume of PBS. After enzyme administration, the animals were monitored daily and clinical signs (hunched posture, decreased activity and rough coat) were noted if observed. All animals were euthanized at the end of day 4 (96 hours). Blood was collected via cardiac puncture and 30 µL of blood was used to perform hematological analysis (Vetscan® HM5 Hematology Analyzer ; Abaxis). The remaining blood was centrifuged in heparin-coated tubes (2,000 × g, 10 minutes, 4°C) for plasma preparation. Biochemical analysis (VetScan® VS2 Chemistry Analyzer ; Abaxis) using the VetScan® Comprehensive Diagnostic Profile (Abaxis) was performed on this plasma.

In vivo treatment of a SUP-B15 cell line xenograft model with L-ASNases

NSG (#005557, the Jackson Laboratory) female mice (n=15) were intravenously injected at 6 weeks of age with 150 µL PBS containing 5×10^6 luciferase-positive SUP-B15 cells. At regular time points, the bioluminescence was measured using the IVIS Lumina II imaging system (PerkinElmer). After evidence of leukemic cell engraftment in the spleen and/or bone marrow, the mice were randomly divided into a vehicle PBS (n=5), PEG-asparaginase (n=5) and ABD-*Er*A-TM (n=5) treatment group. PEG-asparaginase was administered every 10 days via intraperitoneal injection at a dose of 2500 IU/kg (total of 5 administration/doses), while ABD-*Er*A-TM was given at the same dose every 7 days (total of 7 administration/doses). Vehicle mice received the same volume of PBS. During the experiment, leukemic burden was evaluated via bioluminescent imaging (BLI) at regular time points. In addition, body weight was closely monitored. For the AA level determinations in the SUP-B15 xenograft experiment, 120 µL of peripheral blood was collected via a cut in the tail vein 24h after each L-ASNase administration/dose at days 0, 6 and 27 for the ABD-*Er*A-TM treated mice and days 0, 9 and 29 for the PEG-asparaginase mice (n=5). For the activity determinations in the SUP-B15 xenograft experiment, 50 µL of peripheral blood was collected 24h after each L-ASNase administration/dose at days 1, 8, 15, 22, 36 and 43 for the ABD-*Er*A-TM mice and days 1, 11, 21 and 41 for the PEG-asparaginase treated mice (n=5). After treatment, mice were followed up for survival up to day 204 via BLI. On day 204 post treatment initiation, all mice were

sacrificed and the % of human CD45+ cells in the blood, spleen and bone marrow were analyzed by staining with a FITC-labeled antibody for human CD45 (130-114-569; Miltenyi Biotec), performing red blood cell (RBC) lysis and measuring the percentage on a LSRII flow cytometer using FACSDiva software (BD Biosciences).

1. Nguyen HA, Su Y, Lavie A. Design and Characterization of Erwinia Chrysanthemi l-Asparaginase Variants with Diminished l-Glutaminase Activity. J Biol Chem. 2016 Aug 19;291(34):17664-76.
2. Fernandez CA, Cai X, Elozory A, Liu C, Panetta JC, Jeha S, Molinelli AR, Relling MV. High-throughput asparaginase activity assay in serum of children with leukemia. Int J Clin Exp Med. 2013;6(7):478-87.
3. Hejazi M, Piotukh K, Mattow J, Deutzmann R, Volkmer-Engert R, Lockau W. Isoaspartyl dipeptidase activity of plant-type asparaginases. Biochem J. 2002 May 15;364(Pt 1):129-36.
4. Nguyen HA, Su Y, Zhang JY, Antanasijevic A, Caffrey M, Schalk AM, Liu L, Rondelli D, Oh A, Mahmud DL, Bosland MC, Kajdacsy-Balla A, Peirs S, Lammens T, Mondelaers V, De Moerloose B, Goossens S, Schlicht MJ, Kabirov KK, Lyubimov AV, Merrill BJ, Sauntharajah Y, Van Vlierberghe P, Lavie A. A Novel l-Asparaginase with low l-Glutaminase Coactivity Is Highly Efficacious against Both T- and B-cell Acute Lymphoblastic Leukemias In Vivo. Cancer Res. 2018 Mar 15;78(6):1549-1560.